Calculation of desorption and migration of hydrogen on SiGe(100)-2×1 surface using density functional theory

Chia-Liang Cheng[#], Dah-Shyang Tsai, Jyh-Chiang Jiang
[#] presenting author
Department of Chemical Engineering, National Taiwan University of Science and Technology,
43, Keelung Road, Section 4, Taipei 106, Taiwan

Abstract

Ab initio calculations have been carried out to investigate the H-atom migration and H_2 desorption on the mixed SiGe(100)-2×1 surface using the $Si_{9-x}Ge_xH_{13}$, $Si_{14}GeH_{19}$ and $Si_{13}Ge_2H_{19}$ cluster models. The H_2 recombinative desorption is the rate-determining step in hydrogen migration and desorption on SiGe(100) surface since the energy barrier of H-atom migration is generally lower than that of H_2 desorption. Nonetheless H-atom migration into the interdimer position or onto the Ge site still affect the overall pathway and the surface reactivity because its following desorption step is made easier. The Ge presence on surface is interesting, the energy barriers for H_2 desorption from the interdimer, the Si-Ge pair 52.8 kcal/mol and the Ge-Ge pair 45.1 kcal/mol, are lower than that for the Si-Si pair by 7.5 and 15.2 kcal/mol. In other words, the SiGe(100)-2×1 surface in chemical vapor deposition provides more dangling bonds than the Si(100)-2×1 surface owing to the inclusion of Ge.

Introduction

Owing to the benefit of achieving band-gap engineering at lower costs through employing Si-based technology, $Si_{1-x}Ge_x$ epitaxial growth has been integrated into the fabrication processes for high-speed devices, which were restricted to □-V technology previously.[1,2] In the literature, $Si_{1-x}Ge_x$ epitaxial techniques, using ultrahigh vacuum chemical vapor deposition (UHVCVD)[3], rapid thermal chemical vapor deposition (RTCVD)[4] and gas-source molecular beam epitaxy (GSMBE)[5], have been extensively studied. The growing surface in $Si_{1-x}Ge_x$ CVD is generally covered with chemisorbed hydrogen since Si and Ge hydrides are precursors and H_2 gas is commonly employed as the carrier gas. The chemisorbed hydrogen is known to play an important role in the surface reactions of Si growth, which proceeds with the precursor impingement on the site without being covered by hydrogen.[6] The interaction between hydrogen and SiGe surfaces is not only a crucial process in SiGe epitaxies but also one of the most well-defined adsorbate/surface systems.[7] Still many details of hydrogen interaction with SiGe crystalline surfaces remain unknown.

Cluster models are frequently used in studying various processes involving the interactions between gas molecules and crystalline surface. An example which attracts

considerable experimental and theoretical interest over the past years is the dissociative adsorption and associative desorption on the Si(100)-2×1 surface.[8,9] The Si(100)-2×1 surface consists of parallel rows of dimers, with each Si atom of a dimer pair having a dangling bond or a chemisorbed H. The migration of H-atom on the Si(100)-2×1 surface is intimately related to which reaction sites are available. Theoretical calculations using the cluster model have reported activation energies of hydrogen migration on the Si(100)- and Ge(100)-2×1.[10] Owing to the difference in implemented constraints and cluster sizes, the calculated results are dissimilar. Thomsen et al. have summarized the experimental results of SiH_4 growth rates on Si(100), and showed that at low temperature the growth rate is limited by hydrogen desorption and independent of the partial pressure of silane.[7] An activation energy 42 ± 6 kcal/mol of hydrogen desorption has been suggested. This value of hydrogen desorption is quite close to the results measured using the temperature programmed desorption technique under high vacuum condition, 47±3 kcal/mol.[11] The $Si_{1-x}Ge_x$ epitaxial growth mechanism at low Ge contents in CVD has been suggested to be also controlled by the hydrogen desorption reaction. Meanwhile, the correlated activation energy of $Si_{1-x}Ge_x$ growth rate was reduced by the Ge content. Jang and Reif have published results on $Si_{1-x}Ge_x$ epitaxial layer growth.[12] They have deposited $Si_{1-x}Ge_x$ layers using silane-germane gas mixtures at very low pressure. These researchers have suggested a surface-related growth mechanism controlled by hydrogen desorption in the range of low germanium contents. Additional Ge incorporation into $Si_{1-x}Ge_x$ layer would also change the growth rate activation energy of $Si_{1-x}Ge_x$ alloy.

In this article, the H-atom migration and H_2 desorption are simulated using density functional theory (DFT) on SiGe clusters of two sizes. The energetics of these processes are calculated and steps of relatively low energy barriers are identified and connected to be the probable path in the interaction between hydrogen and SiGe surface. Comparison of the results on SiGe and Si surfaces reveals the influence of Ge involvement.

Methodology

Various sizes clusters $Si_{9-x}Ge_xH_{13}$(x=0,1,2), $Si_{14}GeH_{19}$, $Si_{13}Ge_2H_{19}$(I), $Si_{13}Ge_2H_{19}$(II), $Si_{13}Ge_2H_{19}$(III), illustrated in Fig. 1, are used in modeling hydrogen surface migration and combinative desorption. These seven clusters which provide different types of surface atom pairs represent the reconstructed SiGe(100)-2×1 surface. Hydrogen atoms are used to terminate the subsurface dangling bonds of the cluster and keep the tetrahedral structure. The clusters shown in Fig. 1 have been optimized twice. The first optimization is done on the clusters with all dangling bonds being H-terminated. The second optimization is done on the optimized clusters with the one or three hydrogen atoms removed from the surface Si or Ge atom, which represent the surfaces of high and low hydrogen coverage. In the first optimization, the initial bond lengths of the H-atoms to the Si or Ge-atoms have been set to be 1.48 and 1.51 Å. The Si-Si bond length is set to that in bulk silicon, 2.35 Å.

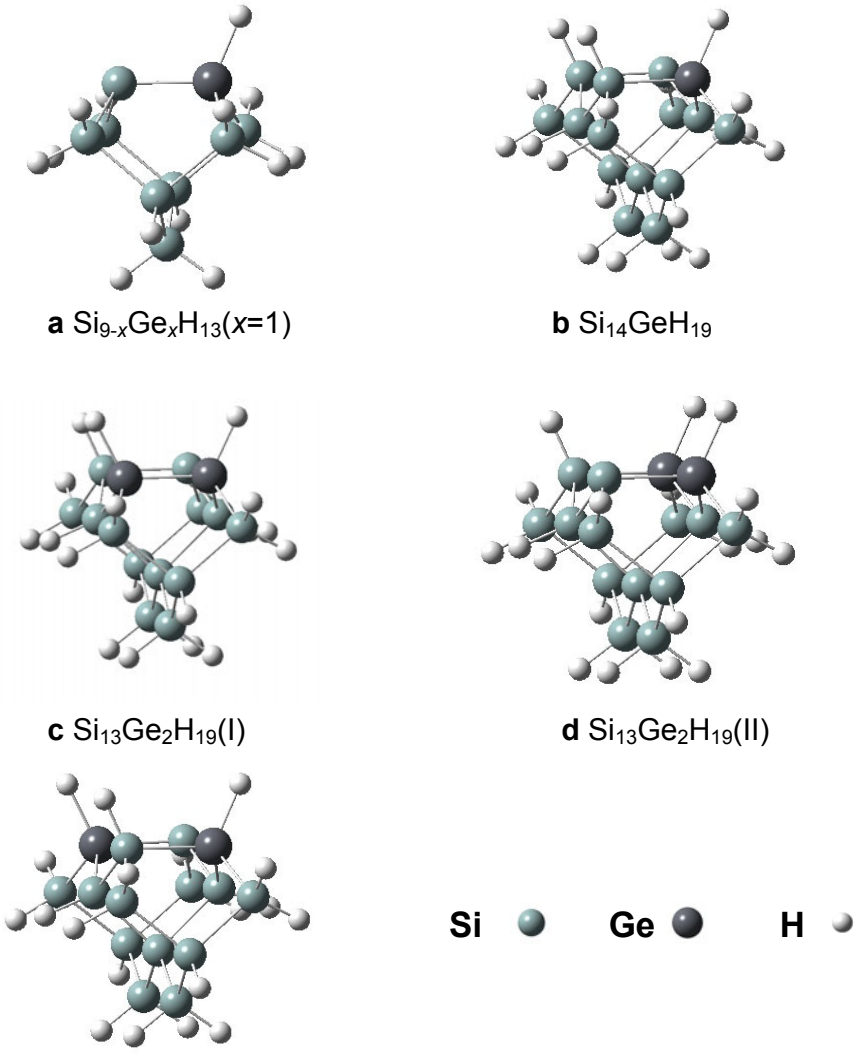

Figure 1. The $Si_{9-x}Ge_x$-H_{13}(x=1), $Si_{14}Ge$-H_{19}, $Si_{13}Ge_2$-H_{19}(I), $Si_{13}Ge_2$-H_{19}(II) and $Si_{13}Ge_2$-H_{19}(III) clusters. The large black atoms are Ge, the small gray atoms are Si, the smallest white atoms are H.

In simulating H-migration on the SiGe(100)-2×1 and Si(100)-2×1 surfaces, three types of H-atom migration to its neighboring site are frequently considered. They are intradimer, interdimer, and interrow jumps, illustrated in Fig. 2. The intradimer migration is the hydrogen jump within the dimer pair, which is simulated on $Si_{9-x}Ge_xH_{13}$(x=0,1,2), $Si_{14}GeH_{19}$, $Si_{13}Ge_2H_{19}$(I), $Si_{13}Ge_2H_{19}$(II) and $Si_{13}Ge_2H_{19}$(III). The interdimer migration is the hydrogen jump between two neighboring dimers in a row, simulated on $Si_{14}Ge$-H_{19}, $Si_{13}Ge_2$-H_{19}(I), $Si_{13}Ge_2$-H_{19}(II) and $Si_{13}Ge_2$-H_{19}(III). The interrow migration is the hydrogen jump between two parallel dimers. The interrow jump is not considered in this article. In simulating the recombinative desorption of hydrogen, two surface H-atoms are considered in the clusters of $Si_{9-x}Ge_xH_{13}$(x=0,1,2). For the clusters of four surface sites, $Si_{14}GeH_{19}$, $Si_{13}Ge_2H_{19}$(I), $Si_{13}Ge_2H_{19}$(II) and $Si_{13}Ge_2H_{19}$(III), the recombinative desorption occurs between two out of

three surface H-atoms.

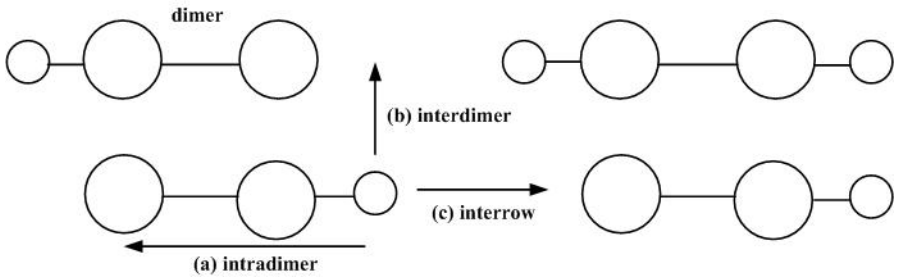

Figure 2. Schematic diagram of the three possible pathways for a migrating H-atom. The H-atom jumps to (a) the other end of the dimer, (b) another dimer in the same row, or (c) a dimer in an adjacent row. Large and little circles denote the surface Si (or Ge) and adsorbed H, respectively.

All computations employ the DFT method with the B3LYP exchange-correlation functional. B3LYP functional has been demonstrated to give reliable predictions for reactions on group-IV semiconductor surfaces. The basis set is the standard all-electron split-valence basis set 6-31G(d), including the polarization d-function for non-hydrogen atoms. Geometry optimizations are performed without artificial geometric constraints. Unscaled zero-point-energies are evaluated at the same level. The transition state (TS) structure is obtained by following a pseudo-reaction coordinate, and the fist-order saddle point is located using the Berny transition-state algorithm. All calculations were performed on HP zx6000 workstations using the Gaussian 98 program software.[13]

Results and discussion

H_2 recombinative desorption. The calculated results of hydrogen recombinative desorption are summarized in Table 1. Values of desorption energy barriers E_d from the intradimer in $Si_{9-x}Ge_xH_{14}$ (x=0, 1 and 2) clusters suggest that desorption from the Si-Si dimer is the most difficult while that from the Si-Ge dimer is easiest, $E_{d,Si\text{-}Ge} < E_{d,Ge\text{-}Ge} < E_{d,Si\text{-}Si}$. On the other hand, values of E_d calculated on the larger clusters, $Si_{14}Ge\text{-}H_{19}$, $Si_{13}Ge_2\text{-}H_{19}$(I), $Si_{13}Ge_2\text{-}H_{19}$(II), $Si_{13}Ge_2\text{-}H_{19}$(III), indicate a different trend. For H_2 desorption from the intradimer pairs, the energy barrier for the Ge-Ge dimer is the smallest of the three, $E_{d,Ge\text{-}Ge} < E_{d,Si\text{-}Ge} < E_{d,Si\text{-}Si}$. The same trend can be seen in the energy barriers of H_2 desorption from the interdimer pairs. The three conceivable $E_{d,Si\text{-}Si}$ barriers of interdimer are 60.3, 60.3 and 60.4 kcal/mol. The six probable $E_{d,Si\text{-}Ge}$ barriers of interdimer are 52.8, 52.7, 52.6, 53.2, 52.7 and 52.8 kcal/mol. The only conceivable $E_{d,Ge\text{-}Ge}$ barrier of interdimer is 45.1 kcal/mol. The calculation results of the larger clusters of 15 SiGe atoms are considered more accurate, since the influence between two dimers is considered in the clusters of 15 SiGe atoms but not in the clusters of 9 SiGe atoms.[10] In view of this cluster size factor and the calculation power of current computer, our discussion will be focused on the results of the clusters consisting 15 SiGe atoms.

TABLE 1: Desorption energy barrier E_d and desorption energy ΔE_{rxn} of intradimer and interdimer path on different clusters (calculated at B3LYP/6-31G(d) level)

Cluster	type	Pair	E_d(kcal/mole)	ΔE_{rxn} (kcal/mole)*
Si_9H_{14}	intradimer	Si-Si	75.8	50.8
Si_8GeH_{14}	intradimer	Si-Ge	57.0	30.6
$Si_7Ge_2H_{14}$	intradimer	Ge-Ge	62.9	34.8
$Si_{14}GeH_{19}$	intradimer	Si-Ge	70.2	40.2
$Si_{14}GeH_{19}$	intradimer	Si-Ge	68.2	40.4
$Si_{14}GeH_{19}$	intradimer	Si-Si	79.4	50.8
$Si_{14}GeH_{19}$	intradimer	Si-Si	73.7	50.3
$Si_{13}Ge_2H_{19}$(I)	intradimer	Ge-Ge	60.9	33.4
$Si_{13}Ge_2H_{19}$(I)	intradimer	Si-Si	74.0	49.5
$Si_{13}Ge_2H_{19}$(II)	intradimer	Si-Ge	68.0	40.4
$Si_{13}Ge_2H_{19}$(II)	intradimer	Si-Ge	66.2	44.8
$Si_{13}Ge_2H_{19}$(III)	intradimer	Si-Ge	67.6	40.2
$Si_{13}Ge_2H_{19}$(III)	intradimer	Si-Ge	67.9	40.4
$Si_{14}GeH_{19}$	interdimer	Si-Ge	52.8	40.0
$Si_{14}GeH_{19}$	interdimer	Si-Ge	52.7	43.6
$Si_{14}GeH_{19}$	interdimer	Si-Si	60.3	48.2
$Si_{14}GeH_{19}$	interdimer	Si-Si	60.3	50.8
$Si_{13}Ge_2H_{19}$(I)	interdimer	Si-Ge	52.6	44.1
$Si_{13}Ge_2H_{19}$(I)	interdimer	Si-Ge	53.2	40.9
$Si_{13}Ge_2H_{19}$(II)	interdimer	Ge-Ge	45.1	34.9
$Si_{13}Ge_2H_{19}$(II)	interdimer	Si-Si	60.4	48.8
$Si_{13}Ge_2H_{19}$(III)	interdimer	Si-Ge	52.7	40.2
$Si_{13}Ge_2H_{19}$(III)	interdimer	Si-Ge	52.8	41.3
$Si_{14}GeH_{20}$	interdimer	Si-Si	74.5	50.6
$Si_{14}GeH_{20}$	interdimer	Si-Ge	68.2	40.4
$Si_{14}GeH_{20}$	intradimer	Si-Si	59.9	54.8
$Si_{14}GeH_{20}$	intradimer	Si-Ge	56.4	42.9

*ΔE_{rxn} is the potential energy difference between the reactant and the product of recombinative desorption reaction.

The calculated E_d of H_2 desorption from binding a pair out of the three surface hydrogen atoms of $Si_{15-x}Ge_xH_{19}$(x=1,2) suggests that this energy barrier depends on the positions of

two adjacent H-atoms. The energy barrier of interdimer pair is always lower than its corresponding value of intradimer pair. For instance, $E_{d,Si\text{-}Ge}$ of interdimer pair is 52.8 kcal/mol, whereas that of intradimer is 68.0 kcal/mol. Similarly, $E_{d,Ge\text{-}Ge}$ of interdimer pair is 45.1 kcal/mol and that of intradimer 60.9 kcal/mol. The site dependence also holds true for H_2 desorption from four surface hydrogen atoms of $Si_{14}GeH_{20}$. The $E_{d,Si\text{-}Ge}$ value of interdimer pair is 56.4 kcal/mol, while that of intradimer pair is 68.2 kcal/mol. The higher energy barrier of intradimer pair is owing to the distortion of TS structure in desorption.

TABLE 2: Energy barrier ($E_{Ge\rightarrow Si}$, $E_{Si\rightarrow Ge}$, $E_{Si\rightarrow Si}$, $E_{Ge\rightarrow Ge}$) (in kcal/mole) of intradimer and interdimer migration on different clusters, and the energy difference ΔE (in kcal/mole) between two directions of H-atom migration in Si-Ge pair (calculated at B3LYP/6-31G(d) level).

Cluster	type	$E_{Ge\rightarrow Si}$	$E_{Si\rightarrow Ge}$	$E_{Si\rightarrow Si}$	$E_{Ge\rightarrow Ge}$	ΔE[a]
Si_9H_{13}	intradimer			38.2		
Si_8GeH_{13}	intradimer	35.1	40.9			-5.8
$Si_7Ge_2H_{13}$	intradimer				34.8	
$Si_{14}GeH_{17}$	intradimer	34.6	40.0			-5.4
$Si_{14}GeH_{19}$	intradimer	34.8	40.6			-5.8
$Si_{14}GeH_{19}$	intradimer			38.0(38.1)		
$Si_{13}Ge_2H_{19}$(I)	intradimer			38.1		
$Si_{13}Ge_2H_{19}$(I)	intradimer				34.2	
$Si_{13}Ge_2H_{19}$(II)	intradimer	34.4	40.2			-5.8
$Si_{13}Ge_2H_{19}$(III)	intradimer	34.9	40.8			-5.9
$Si_{14}GeH_{17}$	intradimer	34.5	42.4			-7.9
$Si_{14}GeH_{19}$	interdimer	30.5	36.1			-5.6
$Si_{14}GeH_{19}$	interdimer			36.6(36.9)		
$Si_{13}Ge_2H_{19}$(I)	interdimer	30.3	35.7			-5.4
$Si_{13}Ge_2H_{19}$(II)	interdimer			36.8		
$Si_{13}Ge_2H_{19}$(II)	interdimer				29.7	
$Si_{13}Ge_2H_{19}$(III)	interdimer	30.0	35.9			-5.9
average	intradimer	34.6±0.3	40.5±0.3	38.1±0.1	34.2	
	theoretical	32.0[b]	38.7[b]	33.5[b],40[c], 29.7[d]	24.7[d]	
	experimental			33.4±4.6[e]		
average	interdimer	30.3±0.3	35.9±0.2	36.7±0.1	29.7	
	theoretical			46.3[b],52[c] , 29.1[d]	23.5[d]	
	experimental			38.0±4.6[e]		

a. $\Delta E=E_{Ge\rightarrow Si}-E_{Si\rightarrow Ge}$

b. energies are obtained from ref. 33

c. energies are obtained from ref. 18

d. energies are obtained from ref. 17

e. energies are obtained from ref. 24

Hydrogen migration. Energy barriers involved the H-atom migration on SiGe are listed in Table 2. The hydrogen migration from a Ge-site to another Ge-site appears to be the easiest step in either interdimer or intradimer pair. The activation energy of migration ($E_{Ge\rightarrow Ge}$) in the intradimer is 34.2 kcal/mol, which is 4.5 kcal/mol higher than that of migration in the interdimer. Correspondingly, the H-atom migration from a Si-site to another Si-site also costs more effort in the intradimer, compared with that in interdimer. The energy barrier of intradimer migration ($E_{Si\rightarrow Si}$) is 38.0 - 38.1 kcal/mol. The lower energy barrier of interdimer migration is 36.6 - 36.9 kcal/mol. The small deviation within the intra- or interdimer migration is due to the difference of the dangling bond position. The migration direction between the Si- and Ge-site makes more difference, comparing with those between Si-Si and Ge-Ge. In general, the hydrogen atom jumps from the Si-site to the Ge-site is more difficult than the jump in the opposite direction. The energy barrier difference between the two directions is quite consistent in different pathways, around 5.6 kcal/mol. The energy barrier of intradimer migration ($E_{Si\rightarrow Ge}$) 40.8 - 40.2 kcal/mol, again, is higher than that of interdimer migration 35.7 - 36.1 kcal/mol. Jumping in the reverse direction is easier, with $E_{Ge\rightarrow Si}$ of intradimer migration 34.4 - 34.9 kcal/mol and that of interdimer migration 30.0-30.5 kcal/mol. The significantly lower energy barrier for hydrogen jump from Ge to Si indicates that hydrogen surface atom tends to stay on top of Si rather than Ge. The energy differences in migration direction can also be explained from the calculated Ge-H and Si-H bond dissociation energies, which are 82.0 and 90.6 kcal/mol respectively.[30] The weaker Ge-H bond is a direct consequence of the 4s electron density distribution in Ge, such that less electron density is available to form a covalent bond.

The tendency of hydrogen migration from Ge to Si was experimentally demonstrated on the SiGe thermal annealed surface analyzed using the in-situ infrared absorption spectroscopy by Hirose et al.[31] Nevertheless the question concerning which is the pathway of hydrogen migration is not answered by experiments. A number of theoretical papers have discussed H-atom migration on the Si surface. Okamoto used $Si_{32}H_{28}$ and $Ge_{32}H_{28}$ two cluster models and calculated the H-atom migration on Si(100)-2×1 and Ge(100)-2×1 surfaces with B3LYP functional.[17] He reported the activated energy of intradimer path was 29.7 and that of interdimer 29.1 kcal/mole on Si surface, on the other hand, that of intradimer path 24.7 kcal/mol and that interdimer 23.5 kcal/mol on Ge surface. Nachtigall and Jordan used Si_9H_{13}, $Si_{15}H_{17}$, and $Si_{23}H_{25}$ clusters of partially fixed atom positions to simulate the H-migration on the Si(001)-2×1 surface. They reported the activated energy 40, 52 and 72 kcal/mole for the intradimer, interdimer, and interrow path.[18] Hierlemann et al. used the DFT

based DMOL module to calculate the H-migration on the SiGe(100)-2×1 surface which was modeled by a cluster of 35 SiGe atoms with fixed positions.[32,33] The energy barrier of intradimer path reported was $E_{Si\rightarrow Ge}$ 38.7 kcal/mol, the opposite path $E_{Ge\rightarrow Si}$ 32.0 kcal/mol.

Hydrogen paths consisting of desorption and migration. Hydrogen coverage on the SiGe and Si surfaces has been recognized to be a crucial factor in the deposition kinetics of epitaxial growth in CVD. The dangling bond on surface is much more reactive and important than the surface site covered with hydrogen in reactions. The dangling bond is created by H-atom migration to suitable sites and proceed recombinative desorption. *Ab-initio* calculations are helpful in revealing the details of surface reaction pathways. We shall discuss the hydrogen desorption and scrambling on the clusters containing different amount of Ge in Fig. 1.

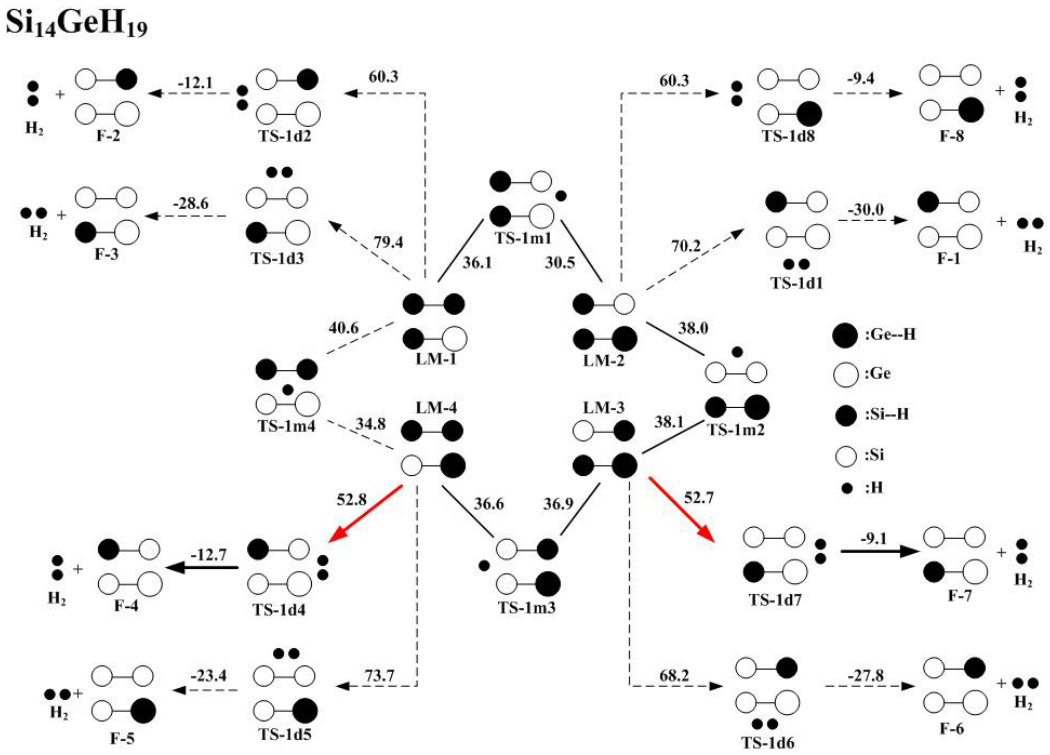

Figure 3. Energy profile diagram of hydrogen migration and desorption on the $Si_{14}GeH_{19}$ cluster. The solid lines represent the most probable paths starting from the configuration LM-1. Energetically, LM-1→TS-1m1→LM-2→TS-1m2→LM-3→TS-1d7→F-7+H_2 is practically the same with LM-1→TS-1m1→LM-2→TS-1m2→LM-3→TS-1m3→LM-4→TS-1d4→F-4+H_2. The big black and white circles represent to monohydride surface Ge-H and Ge vacancies. The medium black and white circles represent to monohydride surface Si-H and Si vacancies. The small black circles represent to hydrogen atoms.

The energy profile diagram of $Si_{14}GeH_{19}$ is illustrated in Figure 3, in which three surface hydrogen atoms can be arranged in four configurations, LM-1, LM-2, LM-3, LM-4. Configuration LM-1, with three surface Si-H bonds and one dangling bond on Ge, is the most

stable one thermodynamically. Its energy after optimization is lower than those of other three configurations by 5.6-5.8 kcal/mol. LM-1 could switch into other configurations via hydrogen scrambling or have a pair of surface hydrogen atoms desorbed. Figure 3 depicts the recombination of two H-atoms of Si-H in LM-1 is more difficult energetically, and the H_2 recombinative desorption demands substantially more energy than hydrogen migration. Thus it is more probable for LM-1 to switch into other configurations containing a Ge-H bond and find a lower H_2-desorption barrier. The scrambling path of LM-1→TS-1m1 →LM-2→TS-1m2→LM-3→TS-1m3→LM-4 consists of lower barriers than that of LM-1→TS-1m4→LM-4. And the energy barrier of H_2 desorption from LM-3 is the most facile step in 8 desorption possible steps. In addition, the desorption barrier of LM-3 52.7 kcal/mol is indistinguishable from that of LM-4 52.8 kcal/mol. Therefore, the paths of LM-1→ TS-1m1→LM-2→TS-1m2→LM-3→TS-1d7→F-7+H_2 and LM-1→TS-1m1→LM-2→ TS-1m2 →LM-3→TS-1m3→LM-4→TS-1d4→ F-4+H_2 are the most probable pathways in hydrogen scrambling and desorption of $Si_{14}GeH_{19}$.

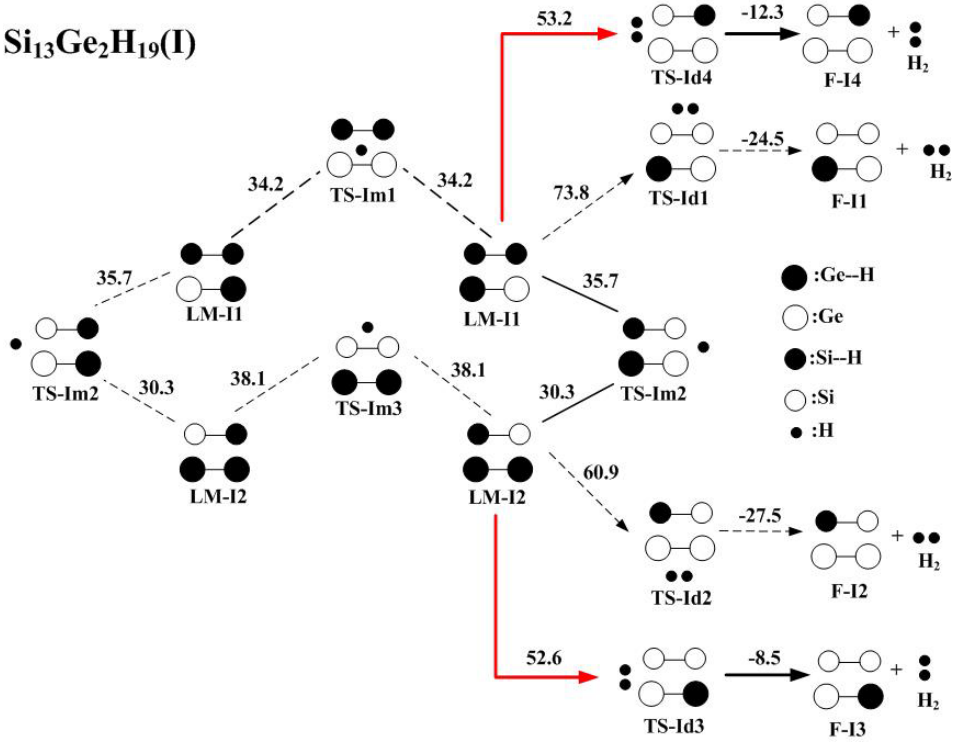

Figure 4. Energy profile diagram of hydrogen migration and desorption on $Si_{13}Ge_2H_{19}$(I) cluster. The solid lines represent the most probable paths starting from the configuration LM-I1. Energetically, the path LM-I1→TS-Id4→F-I4+H_2 is almost the same with LM-I1→TS-Im2 →LM-I2→TS-Id3→F-I3+H_2.

Likewise, the discussion on hydrogen scrambling and desorption of $Si_{13}Ge_2H_{19}$(I) begins with the most stable configuration LM-I1. The most probable pathways in $Si_{13}Ge_2H_{19}$(I) are LM-I1→TS-Id4→F-I4+H_2 and LM-I1→TS-Im2→LM-I2→TS-Id3→ F-I3+H_2, Fig. 4. The most stable configuration of $Si_{13}Ge_2H_{19}$(II) is LM-II2. The most plausible pathway in $Si_{13}Ge_2H_{19}$(II) is LM-II2→TS-IIm1→LM-II1→ TS-IId1→F-II1+H_2, Fig.5. The most stable configuration of

$Si_{13}Ge_2H_{19}$(III) is LM-III2. The most plausible pathways in $Si_{13}Ge_2H_{19}$(III) are LM-III2→ TS-IIId3→F-III3+H_2 and LM-III2→TS-IIIm2 →LM-III1→TS-IIId1→F-III1+H_2, Fig. 6.

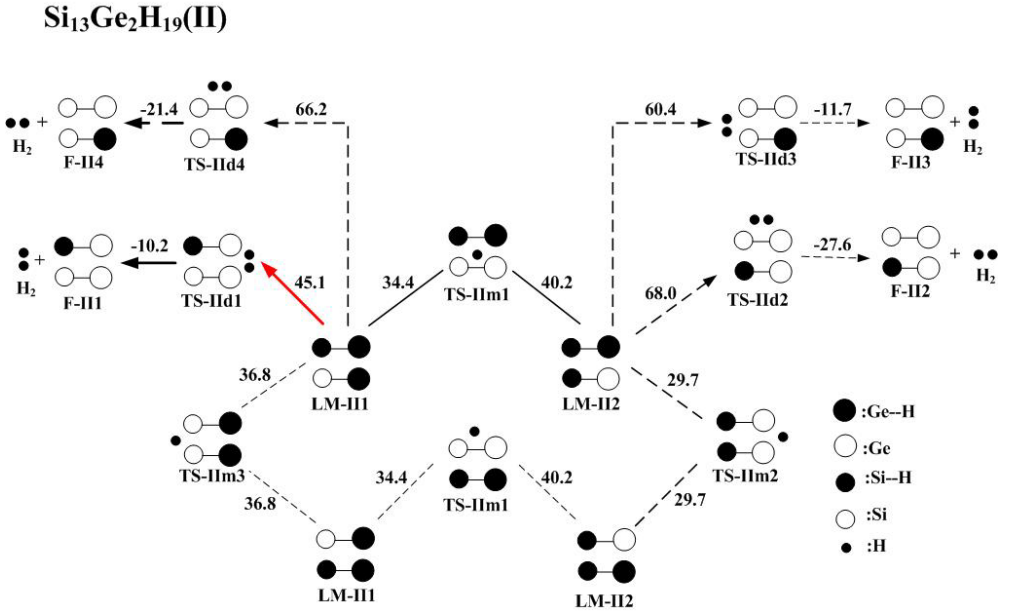

Figure 5. Energy profile diagram of hydrogen scrambling and desorption on $Si_{13}Ge_2H_{19}$(II) cluster. The solid lines represent the most probable path starting from the configuration LM-II2. Energetically, the path LM-II2→TS-IIm1→LM-II1→TS-IId1→F-II1+H_2 is the most probable path.

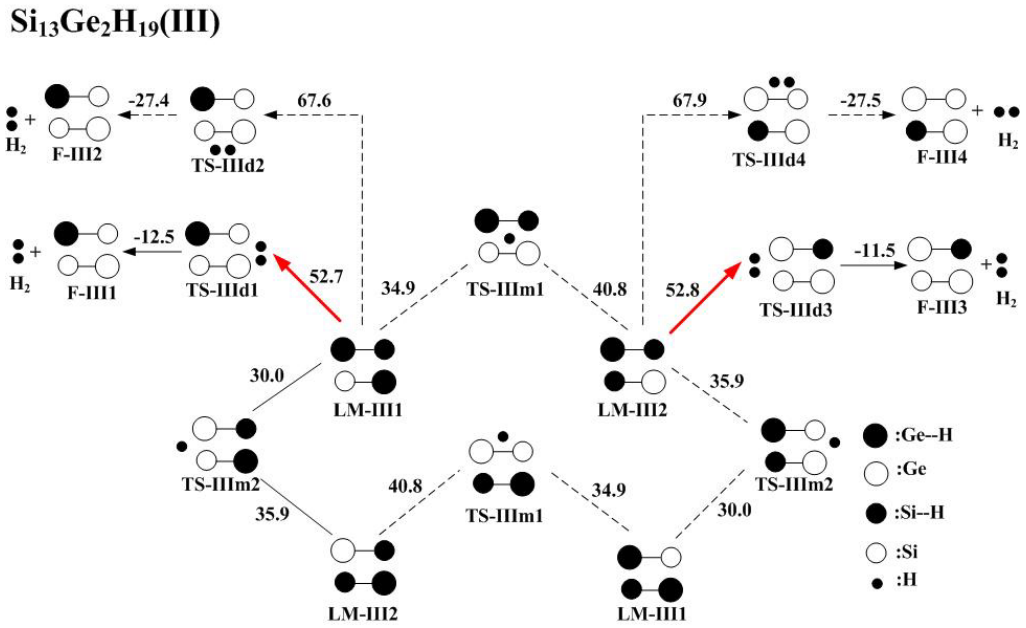

Figure 6. Energy profile diagram of hydrogen scrambling and desorption on $Si_{13}Ge_2H_{19}$(III) cluster. The solid lines represent the most probable paths starting from the configuration LM-III2. Energetically, the path LM-III2→TS-IIId3→F-III3+H_2 is essentially the same with LM-III2→TS-IIIm2 →LM-III1→TS-IIId1→F-III1+H_2.

For hydrogen desorption, the Ge incorporation in Si(100) surface reduces the energy

barrier considerably. It means that hydrogen atoms shall scramble to the Si-Ge and Ge-Ge interdimer pairs, and desorb from there. However, we shall also consider that hydrogen on the Ge site tends to migrate to the Si site. That means that not many Si-Ge and Ge-Ge interdimer pairs are covered by hydrogen. If the SiGe epitaxial growth is in the Si-rich regime, which is also the regime of industrial interest, the Si-Ge pairs shall outnumber the Ge-Ge pairs. The migration from Si to Ge-site requires 35.7-40.7 kcal/mol is higher than that for Ge to Si-site 30.0-34.9 kcal/mol, but still lower than the desorption energy of Si-Ge pairs 52.6-52.8 kcal/mol. Therefore, the H_2 desorption from Si-Ge still is the rate-controlling step. And the growth rate enhancement at low Ge contents found in CVD experiments ought to be attributed to the reduction in energy barrier of H_2 desorption from Si-Ge pairs.

Conclusions

We have studied the hydrogen migration and desorption on the $Si_{1-x}Ge_x$(100)-2×1 surface with various hydrogen coverage, using *ab initio* calculation. The germanium inclusion reduces the energy barriers for hydrogen migration and desorption. Nonetheless the energy barriers of H_2 recombinative desorption reactions are still higher than those of migration and they are the rate-determining steps. Connecting the calculation results of migration and desorption, we find that H-atom often migrates to a position in the interdimer consisting of a surface Ge so that H_2 molecule can recombine more easily and desorb. If there is a Ge-Ge pair on the interdimer position, it will be even more appropriate for hydrogen to move in and desorb. Thus the experimental finding of growth rate enhancement due to Ge incorporation in CVD can be explained by the lowering of energy barriers for hydrogen desorption, which produces a more reactive growing surface.

Acknowledgement

The authors would like to thank the financial support of National Science Council of Taiwan through project NSC 93-2214-E011-001.

References

(1) Szweda, R.; *III-Vs Review* **2003**, 16, 34 .

(2) Meyerson, B. S.; Uram, K. J.; LeGoues F. K. *Appl. Phys. Lett.* **1988**, 53, 2555.

(3) Greve, D. W.; Racanelli, M. *J. Vac. Technol. B* **1990**, 8, 511.

(4) Gu, S.; Zheng, Y.; Zhang, R.; Wang, R. *Physica B* **1996**, 229, 74.

(5) Gao, F.; Huang D. D.; Li, J. P.; Lin, Y. X.; Kong M. Y.; Li, J. M.; Zeng, Y. P.; Lin, L. Y. *J. Crystal Growth* **2000**, 220, 457.

(6) Greve, D. W. *Mater. Sci. Eng. B* **1993**, 18, 22.

(7) Thomsen, E. V.; Christensen, C.; Andersen, C. R.; Pedersen, E. V.; Egginton, P. N.; Hansen, O.; Petersen J. W. *Thin Solid Films* **1997**, 294, 72.

(8) Kolasinski, K. *Int. J. Mod. Phys. B* **1995**, 9, 2753.

(9) Penev, E.; Kratzer, P.; Scheffler, M. *J. Chem. Phys.* **1999**, 110, 3986.

(10) Okamoto, Y. *J. Phys. Chem. B* **2002**, 106, 570.

(11) Sinniah, K.; Sherman, M. G.; Lewis, L. B.; Weinberg, W. H.; Yates, J. T. Jr.; Janda K. C. *Phys. Rev. Lett.* **1989**, 62, 567.

(12) Jang, S. M.; Reif, R. *Appl. Phys. Lett.* **1991**, 59, 3162.

(13) Gaussian 98, revision x.x; Gaussian, Inc.: Pittsburgh, PA, 1998.

(14) Mui, C.; Han, J. H.; Wang, G. T.; Musgrave, C. B.; Bent, S. F. *J. Am. Chem. Soc.* **2002**, 124, 4027.

(15) Hirose, F.; Sakamoto, H.; Terashi, M.; Kuge, J.; Niwano, M. *Thin solid Films* **1999**, 343-344, 404.

(16) Hierlemann, M.; Werner, C. *Materials Science in Semiconductor Processing* **2000**, 3, 31.